Polymer Journal (2015) 47, 282–285

www.nature.com/pj

NOTE

Atomic force microscopy of thermally renatured xanthan with low molar mass

Yasuhiro Matsuda[1], Fumitada Sugiura[1], Jimmy Wayne Mays[2] and Shigeru Tasaka[1]

Polymer Journal (2015) **47,** 282–285; doi:10.1038/pj.2014.102; published online 19 November 2014

INTRODUCTION

Xanthan is a polysaccharide produced by the bacterium *Xanthomonas campestris*. It is widely used in foods, detergents, cosmetics and so on, to control rheological properties. It is widely accepted that native xanthan forms a double helical structure, and that it loses this structure upon heating (denaturation) and recovers the double helical structure upon cooling its solution (renaturation).[1] Products using xanthan are sometimes subjected to heating and cooling processes, such as during cooking. Structural alterations of xanthan induce rheological changes in xanthan solutions, so it is important to characterize the thermally denatured and renatured xanthan for enhanced understanding of the applications of xanthan. However, the structure of renatured xanthan is still under discussion.

One reason why it is difficult to characterize renatured xanthan is that the structure of renatured xanthan changes depending on the conditions of sample preparation, such as temperature, concentrations of both xanthan and added salt and the molar mass of xanthan.

Liu *et al.*[2–4] conducted static light scattering and optical rotation measurements of xanthan solutions containing 0.01 M of NaCl at 25–80 °C. They explained the temperature dependence of their experimental results by presenting a model in which the helical structure only partially unwinds, but the remaining double helical structure prevents xanthan from dissociating into two random coils. Kawakami *et al.*[5] carried out sedimentation equilibrium, viscosity and optical rotation measurements of xanthan solutions heated upto 95 °C for different periods of time. They detected a decrease in the molar mass of xanthan samples heated for longer than 7 h and an increase in the molar mass after quenching, which reflects the dissociation and aggregation of xanthan during denaturation and renaturation.

Oviatt and Brant,[6] and Capron *et al.*[7] investigated the structure of renatured xanthan, and they proposed models that appear to be inconsistent with one another. Oviatt and Brant,[6] carried out viscoelastic measurements of xanthan samples renatured at relatively high concentration of xanthan (10–30 $g\,l^{-1}$), and they detected enhanced viscosity upon renaturation, which indicates the formation of large aggregates by renaturation. In contrast, Capron *et al.*[7] argued that xanthan dissociates into two random coils during denaturation, and each random coil forms a hairpin-shaped helix during renaturation at a low concentration of xanthan (1 $g\,l^{-1}$).

Using size exclusion chromatography-on line multi angle light scattering (SEC-MALS) and circular dichroism (CD) measurements, we characterized the structure of xanthan samples with molar masses of $1.2–14 \times 10^5$ in their native state, under different denaturation and renaturation conditions.[8] There appears to be two different schemes by which xanthan denatures and renatures, and we propose structures for denatured and renatured xanthan (Figure 1). In solutions with low concentrations of xanthan and added salt, the double helices of xanthan dissociate into two random coils during denaturation. During renaturation, the two random coils recover their helical structure by forming two hairpin-shaped helices with half the contour length of native xanthan. In solutions with relatively high concentration of xanthan and added salt, the helical structure only partially unwinds, and the remaining double helical structure prevents xanthan from dissociating into two random coils. During renaturation, the partially unwound xanthan rewinds with neighboring xanthan to form branched aggregates. The molar mass, molar mass dependence of radius of gyration and CD spectra of the renatured xanthan can all be explained by these proposed models, which strongly supports these models.

While experiments on xanthan solutions have provided *in situ* information on the structure of xanthan, there have been some works on observing xanthan by microscopy to obtain the direct visual evidence of its structure. Pioneering studies of atomic force microscopy (AFM), to study xanthan, were conducted by preparing samples from alcohol solution.[9–11] Electron microscopy has also been used to investigate the global structure and rigidity of xanthan.[12]

AFM was used to characterize the structures of denatured and renatured xanthan. Camesano and Wilkinson,[13] recorded AFM images of the partially unwound or rewound helical structures of xanthan denatured in aqueous solution containing different concentrations of KCl. They also conducted some statistical analyses of the contour length, persistence length and height of xanthan helices. Ikeda *et al.*[14]

[1]Department of Applied Chemistry and Biochemical Engineering, Shizuoka University, Hamamatsu, Japan and [2]Department of Chemistry, The University of Tennessee, Knoxville, Tennessee, USA
Correspondence: Dr Y Matsuda, Department of Applied Chemistry and Biochemical Engineering, Shizuoka University, 3-5-1 Johoku, Naka-ku, Hamamatsu, Shizuoka 432-8561, Japan.
E-mail: matsuda.yasuhiro@shizuoka.ac.jp
Received 7 July 2014; revised 21 September 2014; accepted 26 September 2014; published online 19 November 2014

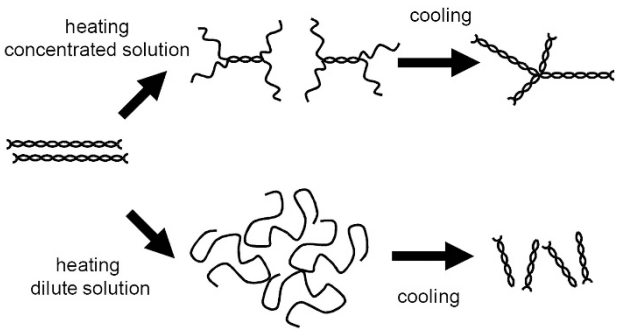

Figure 1 Models of denatured and renatured xanthan proposed in reference 8.

observed native and renatured xanthan by AFM, and they identified a branched structure for a native xanthan sample and network structure for a thermally denatured and renatured xanthan sample.

Both, Camesano and Wilkinson,[13] and Ikeda *el al.*,[14] used commercially available xanthan samples with very high molar mass and wide molar mass distribution. Although, the very high molar mass of commercially available xanthan samples prevent precise determination of their molar mass, their molar masses are believed to be $\sim 10^7$. By using a reported value of molar mass per contour length (1940 nm^{-1}),[15–17] the contour length of commercially available xanthan samples can be calculated as $\sim 5\,\mu m$, which is much higher than the reported value of the persistence length of xanthan (120 nm).[15–17] Because the contour length is much longer than the persistence length, the long xanthan chains in commercially available samples can bend and become entangled in spite of their rigidity, and it explains the complicated structures observed by Ikeda *et al.*[14] in their AFM images. Although, it is important to characterize the structure of commercially available xanthan samples for industrial purposes, these complexities make it difficult to clarify the structure of xanthan.

In this study, we used a xanthan sample that was sonicated to reduce its molar mass and fractionated to narrow the molar mass distribution. This made it possible to obtain clearer evidence of the structures of xanthan sample renatured in solution with different xanthan concentrations, as proposed in our previous paper.[8]

EXPERIMENTAL PROCEDURE

The xanthan sample used in this study was kindly provided by Professor Takahiro Sato of Osaka University. It was prepared by sonication, purification, fractionation and neutralization, the details of which are described in his previous report.[15] The number average molar mass and molar mass distribution index of this sample in the native state were 2.93×10^5 and 1.05, respectively, as measured by SEC-MALS. SEC-MALS measurement was carried out using an aqueous solution containing 0.1 M of NaCl as the eluent at 40 °C. The MALS detector was a Wyatt-199-Rex (Wyatt Technology, Santa Barbara, CA, USA) with 50 mW GaAs laser at a wavelength of 660 nm. The eluent was flowed at $0.8\,ml\,min^{-1}$ with an Agilent 1100 pump (Agilent Technologies, Santa Clara, CA, USA). The specific refractive index increment of xanthan in this eluent was $0.138\,ml\,g^{-1}$, as determined in our previous study.[8] Using the values of molecular weight per contour length, reported in previous studies,[15–17] the contour length was calculated to be 151 nm. Because the persistence length of native xanthan was reported to be 120 nm,[15–17] the double helices of native xanthan in the sample used in this study exist as almost extended rods. The molecular weight dispersion of renatured samples are wider than those of the corresponding native samples.[8] The electrical conductivity of the deionized water used in this study was $1.3\,\mu S\,cm^{-1}$, as measured with an inoLab Cond Level (WTW GmbH, Weiheim, Germany) electrical conductivity meter, which indicates that this water is pure enough for these experiments.

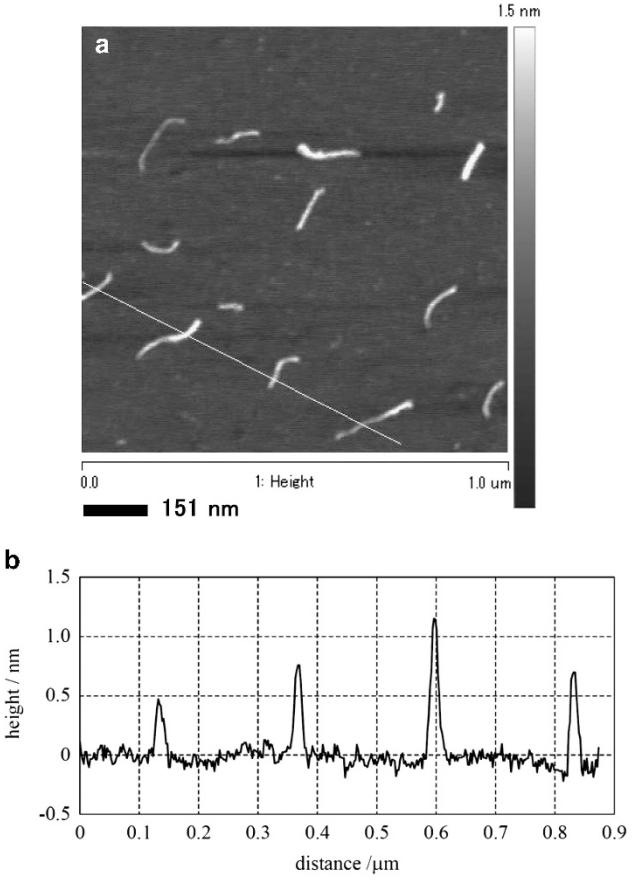

Figure 2 An AFM image of native xanthan (**a**) and the profile of the white line (**b**).

To prepare a native xanthan sample for AFM measurements, the xanthan sample was dissolved in a 0.01 M aqueous solution of NaCl to avoid unintended denaturation. Approximately 2 μl of the solution containing $10^{-2}\,g\,l^{-1}$ xanthan was dropped onto a mica plate with a diameter of 9.9 mm, purchased from Ted Pella, Inc. (Redding, CA, USA), and the solution was dried before taking measurements. The mica plates were freshly cleaved just before dropping the solutions.

Two types of renatured solutions with different concentration of xanthan, during the denaturation and renaturation processes, were prepared. A xanthan solution containing $10\,g\,l^{-1}$ xanthan was prepared by dissolving the sample in deionized water and heating upto 80 °C for 1 h for denaturation. This solution was renatured by adding the same volume of an aqueous solution of 0.2 M of NaCl and allowing it to stand at room temperature for 1 day. A solution containing $10^{-2}\,g\,l^{-1}$ of xanthan was prepared by diluting this solution with 0.01 M aqueous NaCl. This solution was dropped onto a mica plate and dried by the same procedure as used for the native solution. This condition was essentially the same as that for the solution which was reported to induce xanthan to form branched aggregates.[8]

A xanthan solution denatured and renatured under the conditions known to cause the formation of hairpin-shaped helices[8] was also prepared as follows. A solution containing $1\,g\,l^{-1}$ xanthan was prepared by dissolving the sample in deionized water and heating upto 80 °C for 1 h. This solution was renatured by adding the same volume of an aqueous solution of 0.02 M NaCl and allowing it to stand at room temperature for 1 day. The solution containing $10^{-2}\,g\,l^{-1}$ xanthan was prepared by dilution in 0.01 M aqueous NaCl and dropped onto a mica plate and dried by the same procedure as for the native solution.

The AFM instrument and measurement conditions used in this study were the same as those used for another polymer in our previous study, and the details are described in our previous paper.[18]

RESULTS AND DISCUSSION

Figure 2a is an AFM image of native xanthan. Almost extended rods are observed in the image. The black bar below the image indicates the calculated contour length of the sample, and the lengths of the observed rods are comparable with the length of the black bar. Because the contour length was only 1.26 times longer than the persistence length, the almost extended structure of the observed rods is reasonable for the native xanthan used in this study. The profile of the white line in Figure 2a is shown in Figure 2b. The height of the observed rods does not contradict the value reported for double helices of xanthan by Camesano and Wilkinson.[13]

Figure 3a is an AFM image of a xanthan sample that was denatured and renatured at a relatively high concentration of xanthan, and the black bar indicates the contour length of the native sample. Branched rods longer than the contour length of the native sample are observed, and this structure is consistent with the branched chain model that was proposed to explain the experimental results of SEC-MALS and CD spectra in the previous paper.[8] Figure 4a is another AFM image of a xanthan sample that was denatured and renatured at a relatively high xanthan concentration. A long rod with short branched rods is observed, and the length of the long rod is comparable with twice the contour length of the native sample (302 nm), indicated by the black bar. This image is reasonable based upon the aggregates formed by two double helices of xanthan, as proposed in the previous report.[8] Figures 3b and 4b show the profiles of the white lines in the corresponding images. The height of the observed aggregates do not contradict the value reported for double helices of xanthan by Camesano and Wilkinson.[13]

Figure 5a is an AFM image of a xanthan sample that was denatured and renatured at a low concentration of xanthan, and the black bar indicates half of the contour length of the native sample (75 nm). Short extended rods without branching structures are observed, and their lengths are comparable with the length of the black bar. This structure is reasonable for the structure of the hairpin-like helices, which was proposed to explain the experimental results of SEC-MALS and CD spectra in the previous paper.[8] The profile of the white line in

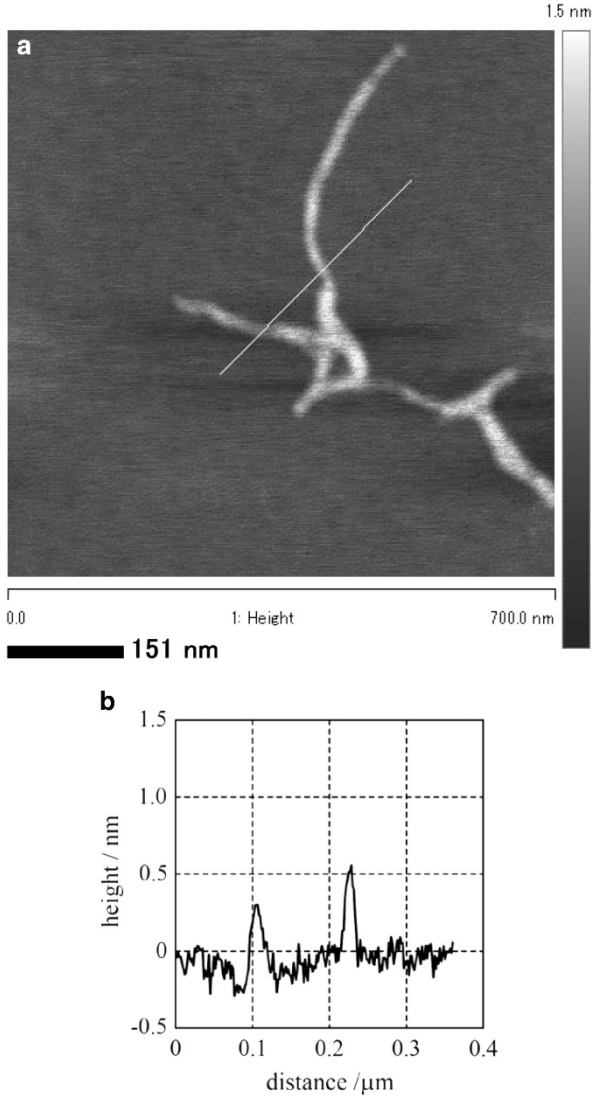

Figure 3 An AFM image of xanthan denatured and renatured at a relatively high concentration of xanthan (**a**) and the profile of the white line (**b**).

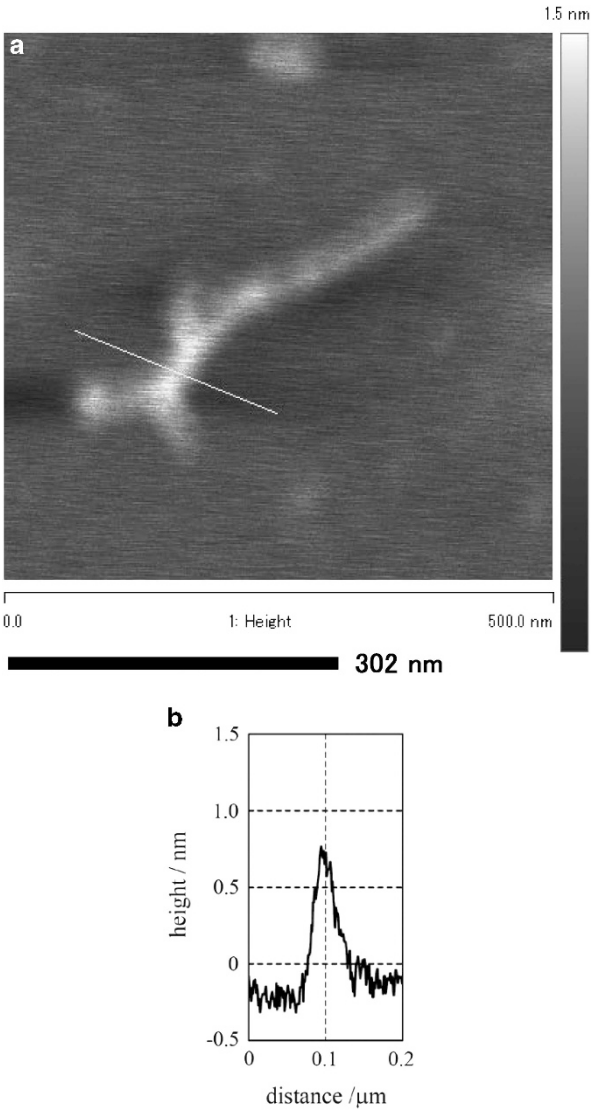

Figure 4 Another AFM image of xanthan denatured and renatured at a relatively high concentration of xanthan (**a**) and the profile of the white line (**b**).

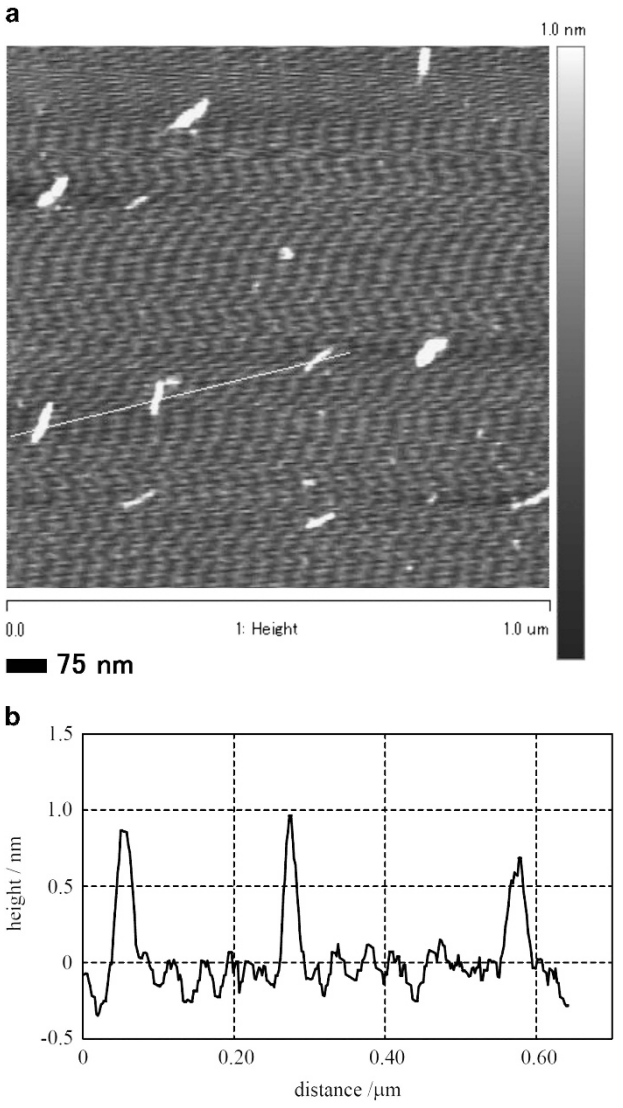

Figure 5 An AFM image of xanthan denatured and renatured at a low concentration of xanthan (**a**) and the profile of the white line (**b**).

the figure is shown in Figure 5b. The height of the observed rods does not contradict the value reported for double helices of xanthan by Camesano and Wilkinson.[13]

The structures observed in AFM images of native xanthan and xanthan samples renatured under different conditions agree well with the models proposed to explain the experimental results of SEC-MALS and CD spectra, as reported in the previous paper.[8] The lengths and heights of the observed images are consistent with the values obtained using the proposed models,[8] and that of double helices reported by Camesano and Wilkinson,[13] respectively. The AFM images shown in this paper strongly support that the proposed models reflect the structures of native and renatured xanthan in solutions.

ACKNOWLEDGEMENTS

We thank Professor Takahiro Sato of Department of Macromolecular Science, Osaka University, for providing his xanthan samples. We are also grateful to Dr. Kunlun Hong of Center for Nanophase Materials Sciences Division, Oak Ridge National Laboratory, and Mr. Weiyu Wang of Department of Chemistry, The University of Tennessee, for their fruitful discussions and help with SEC-MALS measurement. JWM acknowledges partial support from the Division of Materials Science and Engineering, BES, U.S. Department of Energy.

1 Norisuye, T. & Teramoto, A. in *Polymeric Materials Encyclopedia* (ed. Salamone, J. C.) 8801–8809 (CRC Press: Boca Raton, USA, 1996).
2 Liu, W., Sato, T., Norisuye, T. & Fujita, H. Thermally induced conformational change of xanthan in 0.01 M aqueous sodium chloride. *Carbohydr. Res.* **160**, 267–281 (1987).
3 Liu, W. & Norisuye, T. Order-disorder conformation change of xanthan in 0.01 M aqueous sodium chloride: dimensional behavior. *Biopolymers* **27**, 1641–1654 (1988).
4 Liu, W. & Norisuye, T. Thermally induced conformation change of xanthan: interpretation of viscosity behavior in 0.01 M aqueous sodium chloride. *Int. J. Biol. Macromol.* **10**, 44–50 (1988).
5 Kawakami, K., Okabe, Y. & Norisuye, T. Dissociation of dimerized xanthan in aqueous solution. *Carbohydr. Polym.* **14**, 189–203 (1991).
6 Oviatt, H. W. Jr & Brant, D. A. Viscoelastic behavior of thermally treated aqueous xanthan solutions in the semidilute concentration regime. *Macromolecules* **27**, 2402–2408 (1994).
7 Capron, G., Brigand, G. & Muller, G. About the native and renatuerd conformation of xanthan exopolysaccharide. *Polymer* **38**, 5289–5295 (1997).
8 Matsuda, Y., Biyajima, Y. & Sato, T. Thermal denaturation, renaturation, and aggregation of a double-helical polysaccharide xanthan in aqueous solutions. *Polym. J.* **41**, 526–532 (2009).
9 Kirby, A. R., Gunning, A. P. & Morris, V. J. Imaging xanthan gum by atomic force microscopy. *Carbohydr. Res.* **267**, 161–166 (1995).
10 Gunning, A. P., Kirby, A. R. & Morris, V. J. Imaging xanthan gum in air by Ac "Tapping" mode atomic force microscopy. *Ultramicroscopy* **63**, 1–3 (1996).
11 Capron, I., Alexandre, S. & Muller, G. An atomic force microscopy study of the molecular organization of xanthan. *Polymer* **39**, 5725–5730 (1998).
12 Stokke, B. T. & Elgsaeter, A. The molecular size and shape of xanthan, xylinan, bronchial mucin, alginate, and amylose as revealed by electron microscopy. *Carbohydr. Res.* **160**, 13–28 (1987).
13 Camesano, T. A. & Wilkinson, K. J. Single molecule study of xanthan conformation using atomic force microscopy. *Biomacromolecules* **2**, 1184–1191 (2001).
14 Ikeda, S., Gohtani, S., Nishinari, K. & Zhong, Q. Single molecules and networks of xanthan gum probed by atomic force microscopy. *Food Sci. Technol. Res.* **18**, 741–745 (2012).
15 Sato, T., Norisuye, T. & Fujita, H. Double-stranded helix of xanthan in dilute solution: evidence from light scattering. *Polym. J.* **16**, 341–350 (1984).
16 Sato, T., Kojima, S., Norisuye, T. & Fujita, H. Double-stranded helix of xanthan in dilute solution: further evidence. *Polym. J.* **16**, 423–429 (1984).
17 Sato, T., Norisuye, T. & Fujita, H. Double-stranded helix of xanthan in dilute solution: dimensional and hydrodynamic properties in 0.1 M aqueous sodium chloride. *Macromolecules* **17**, 2696–2700 (1984).
18 Matsuda, Y., Fukatsu, A., Wang, Y., Miyamoto, K., Mays, J. W. & Tasaka, S. Fabrication and characterization of poly(L-lactic acid) gels induced by fibrous complex crystallization with solvents. *Polymer* **55**, 4369–4378 (2014).